Decreased lymphatic HIF-2α accentuates lymphatic remodeling in lymphedema

Xinguo Jiang,[1,2] Wen Tian,[1,2] Eric J. Granucci,[1,2] Allen B. Tu,[1,2] Dongeon Kim,[1,2] Petra Dahms,[1,2] Shravani Pasupneti,[1,2] Gongyong Peng,[1,2] Yesl Kim,[1,2] Amber H. Lim,[1,2] F. Hernan Espinoza,[2] Matthew Cribb,[3] J. Brandon Dixon,[3] Stanley G. Rockson,[2] Gregg L. Semenza,[4,5,6,7,8,9,10] and Mark R. Nicolls[1,2]

[1]VA Palo Alto Health Care System, Palo Alto, California, USA. [2]Stanford University School of Medicine, Stanford, California, USA. [3]Georgia Institute of Technology, Atlanta, Georgia, USA. [4]Vascular Biology, Institute for Cell Engineering, [5]Department of Pediatrics, [6]Department of Medicine, [7]Department of Oncology, [8]Department of Radiation Oncology, and [9]Department of Biological Chemistry, and [10]McKusick-Nathans Institute of Genetic Medicine, Johns Hopkins University School of Medicine, Baltimore, Maryland, USA.

Pathologic lymphatic remodeling in lymphedema evolves during periods of tissue inflammation and hypoxia through poorly defined processes. In human and mouse lymphedema, there is a significant increase of hypoxia inducible factor 1 α (HIF-1α), but a reduction of HIF-2α protein expression in lymphatic endothelial cells (LECs). We questioned whether dysregulated expression of these transcription factors contributes to disease pathogenesis and found that LEC-specific deletion of *Hif2α* exacerbated lymphedema pathology. Even without lymphatic vascular injury, the loss of LEC-specific *Hif2α* caused anatomic pathology and a functional decline in fetal and adult mice. These findings suggest that HIF-2α is an important mediator of lymphatic health. HIF-2α promoted protective phosphorylated TIE2 (p-TIE2) signaling in LECs, a process also replicated by upregulating TIE2 signaling through adenovirus-mediated *angiopoietin-1* (*Angpt1*) gene therapy. Our study suggests that HIF-2α normally promotes healthy lymphatic homeostasis and raises the exciting possibility that restoring HIF-2α pathways in lymphedema could mitigate long-term pathology and disability.

Introduction

Lymphedema is characterized by a chronic state of lymphatic vascular insufficiency with interstitial edema, inflammation, and dermal pathology; it affects 100–250 million individuals globally, but lacks effective pharmacological therapies (1–3). Whereas primary lymphedema occurs in either heritable or idiopathic fashion, secondary lymphedema results from acquired lymphatic vascular damage caused by cancer, cancer therapy, parasitic infection, and trauma (4, 5). Despite significant advancements in the last few decades, our knowledge about the pathogenesis and evolution of lymphedema is still incomplete. Pathological lymphatic vascular remodeling is critically implicated in lymphedema progression (6). Elucidating key molecular pathways involved in lymphatic disease and remodeling can facilitate the discovery of much-needed therapeutic targets.

Hypoxia inducible factors (HIFs), particularly HIF-1α and HIF-2α isoforms, are important mediators that govern adaptive responses to tissue hypoxia and inflammation (7–9). While HIF isoforms have substantial structural conservation and regulate some overlapping target genes, they also play distinct, context-dependent and cell-specific roles by controlling the expression of different target gene sets (10, 11). HIFs are well-known to regulate blood vascular growth and remodeling through a number of pathways, including the angiopoietin (ANGPT)/TIE2 cascade (12, 13). This signaling pathway is comprised of 2 main ligands, ANGPT1, ANGPT2, and TIE1, TIE2 receptors; differential interactions of these ligands and receptors mediate a variety of effector functions in vascular biology (14). As regulators of TIE2 signaling, the HIFs are important candidates to evaluate when considering diseases of blood and lymphatic circulatory systems (14–16).

Lymphedema tissue is hypoxic and chronically inflamed (17, 18), and we found that HIF-1α was high but HIF-2α was low in clinical lymphedema skin. We hypothesized that HIFs play a role in modulating lymphatic changes in this disease. To explore this possibility, we employed the mouse-tail subacute lymphedema model, which closely simulates the volume responses, immune infiltration, and skin remodeling observed in clinical disease (17, 19). Using lymphatic endothelial cell–specific (LEC-specific) *Hifα* loss- and gain-of-function transgenic mouse lines, we found that deletion of lymphatic *Hif2α* markedly exacerbated lymphedema compared with gene silencing of *Hif1α*. Even in the absence of lymphatic injury, reduced LEC HIF-2α was associated with pre- and postnatal lymphatic pathology. Conversely, augmenting LEC HIF-2α expression enhanced lymphatic functioning and alleviated lymphedema. Endogenous HIF-2α appears to stabilize LECs through tonic TIE2 activation. Consistently, augmenting lymphatic TIE2 signaling through overexpressing ANGPT1 also alleviates lymphedema. Our study suggests that reduced lymphatic HIF-2α expression contributes to the evolution of lymphedema and that approaches augmenting HIF-2α activity hold therapeutic promise.

Authorship note: XJ, WT, EJG, and ABT are co–first authors.
Conflict of interest: MRN, XJ, and GS are coinventors on a patent for the use of the topical surgical solution that upregulates HIF-1α and HIF-2α for preconditioning transplanted airways ("Iron chelators and the use thereof for reducing transplant failure during rejection episodes," patent no. US 9,763,899).

Submitted: January 3, 2020; **Accepted:** July 9, 2020; **Published:** September 21, 2020.
Reference information: *J Clin Invest*. 2020;130(10):5562–5575.
https://doi.org/10.1172/JCI136164.

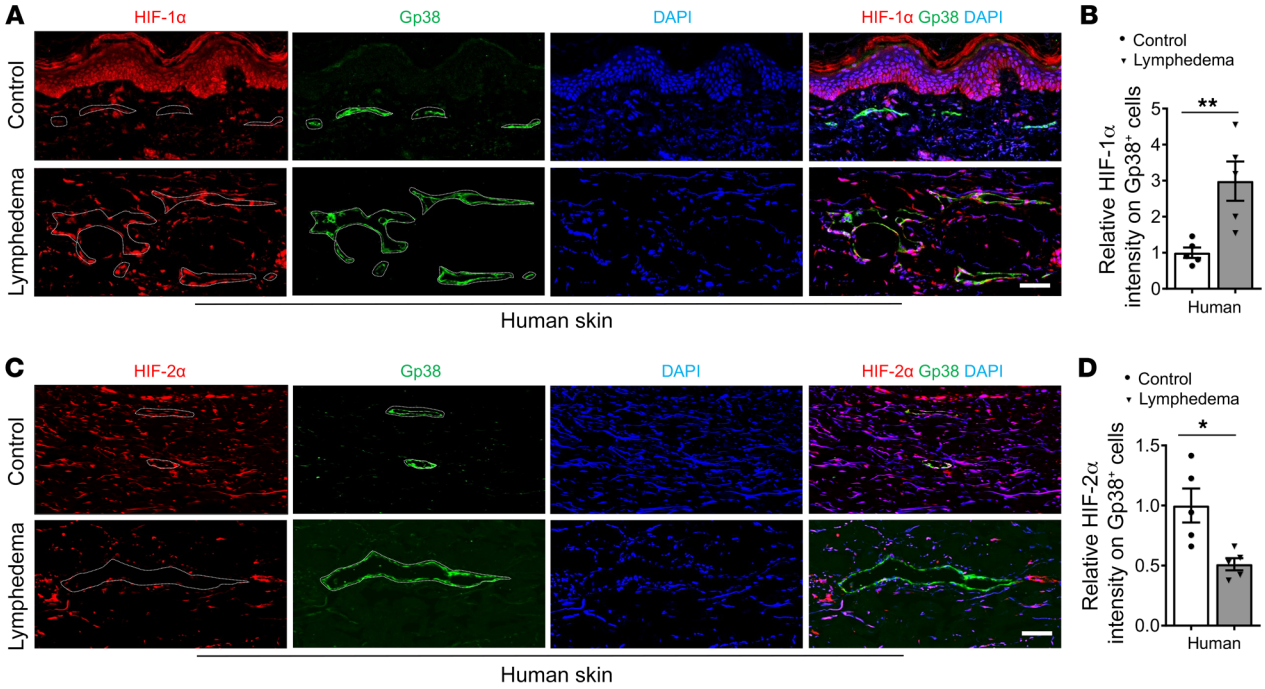

Figure 1. Increased HIF-1α but decreased HIF-2α expression in LECs of human lymphedema skin. (**A**) Representative immunofluorescence staining of HIF-1α (red) and Gp38 (green) in control and lymphedematous clinical samples. DAPI (blue) stains the nucleus. White dashed lines demarcate lymphatics. (**B**) Quantification of HIF-1α intensity comparing groups shown in **A** (n = 5). (**C**) Representative immunofluorescence staining of HIF-2α (red) and Gp38 (green) of human samples. DAPI (blue) stains the nucleus. White dashed lines demarcate lymphatics. (**D**) Quantification of HIF-2α intensity comparing groups shown in **C** (n = 5). In **B** and **D**, data are presented as mean ± SEM; $^*P < 0.05$; $^{**}P < 0.01$; by the Mann-Whitney test. n represents numbers of patients. Scale bars: 60 μm (**A** and **C**).

Results

Lymphedema is characterized by increased LEC HIF-1α but reduced HIF-2α expression. The dermis layer in lymphedema is hypoxic and inflamed, and so we sought to discern how the key regulators of hypoxic responses might be involved. To evaluate the differential roles of HIF-1α and HIF-2α in lymphedema, we first assessed their expression in skin samples of clinical and preclinical lymphedema. Elevated HIF-1α expression in LECs was present in the lymphedematous limbs compared with the lateral control ones (Figure 1, A and B, and Supplemental Figure 1A; supplemental material available online with this article; https://doi.org/10.1172/JCI136164DS1). Conversely, HIF-2α expression was decreased in LECs in human lymphedema (Figure 1, C and D, and Supplemental Figure 1B). These data prompted us to investigate the differential roles of LEC HIF isoforms in the development of lymphedema. We used the mouse-tail model of acquired lymphedema, in which lymphatic dysfunction is induced by ablation of the major lymphatic trunks, whereas the control (sham) operation involves only a skin incision without lymphatic injury (Figure 2A). Lymphedema is quantified by tail volume changes and has a characteristic disease progression phase for the first 2 weeks followed by a disease resolution period (Figure 2B). This murine model of subacute, acquired lymphedema closely simulates the histopathology of human disease with expansion of the dermis and epidermis, and distortion of the epidermal/dermal junction (Figure 2C). Consistent with clinical disease, mouse lymphedema groups showed an increased expression of HIF-1α in LECs compared with the sham controls (Figure 2, D and E). As with the human condition, LEC HIF-2α was decreased in the lymphedematous mouse tails (Figure 2, F and G). These data demonstrate a differential LEC expression pattern of HIFα subunits in lymphedema both in human and mice, suggesting that these HIF isoforms might play divergent roles in regulating lymphatic function with distinct effects on lymphatic pathophysiology in lymphedema.

Inducing the genetic deletion of LEC Hif2α exacerbates lymphatic remodeling and aggravates lymphatic dysfunction in lymphedema. We confirmed that mouse lymphedema skin is hypoxic (11, 18), as assessed by the hypoxyprobe, pimonidazole (Supplemental Figure 2). To test whether LEC HIF isoforms differentially regulate lymphedema pathophysiology, we generated LEC-specific *Hif1α* or *Hif2α* loss-of-function mice by crossing *Prox-1-CreERT2* animals with mice expressing *Hif1α*$^{fl/fl}$ or *Hif2α*$^{fl/fl}$ transgene; reporter mice with *tdTomato* highlighting LECs were also created (Supplemental Figure 3). Whole-mount tail-skin image showed a strong induction of tdTomato, which marked lymphatics following tamoxifen administration, but not in those without tamoxifen exposure (Supplemental Figure 4), indicating the Prox-1 promoter-controlled CreERT2 can effectively mediate gene recombination in a tamoxifen-dependent manner, with negligible spontaneous enzymatic activity of CreERT2 in mouse skin. Immunofluorescence staining further indicated that CreERT2 efficiently mediated the knockout (KO) of *Hif1α* or *Hif2α* genes in LECs (LEC *Hif1α*-KO or LEC *Hif2α*-KO, Supplemental Figures 5 and 6). LEC *Hif1α*-KO also effectively reduced LEC HIF-1α expression in mice subjected to lymphatic surgery (Supplemental Figure 7). However, LEC-specific *Hif1α* deletion only modestly exacerbated

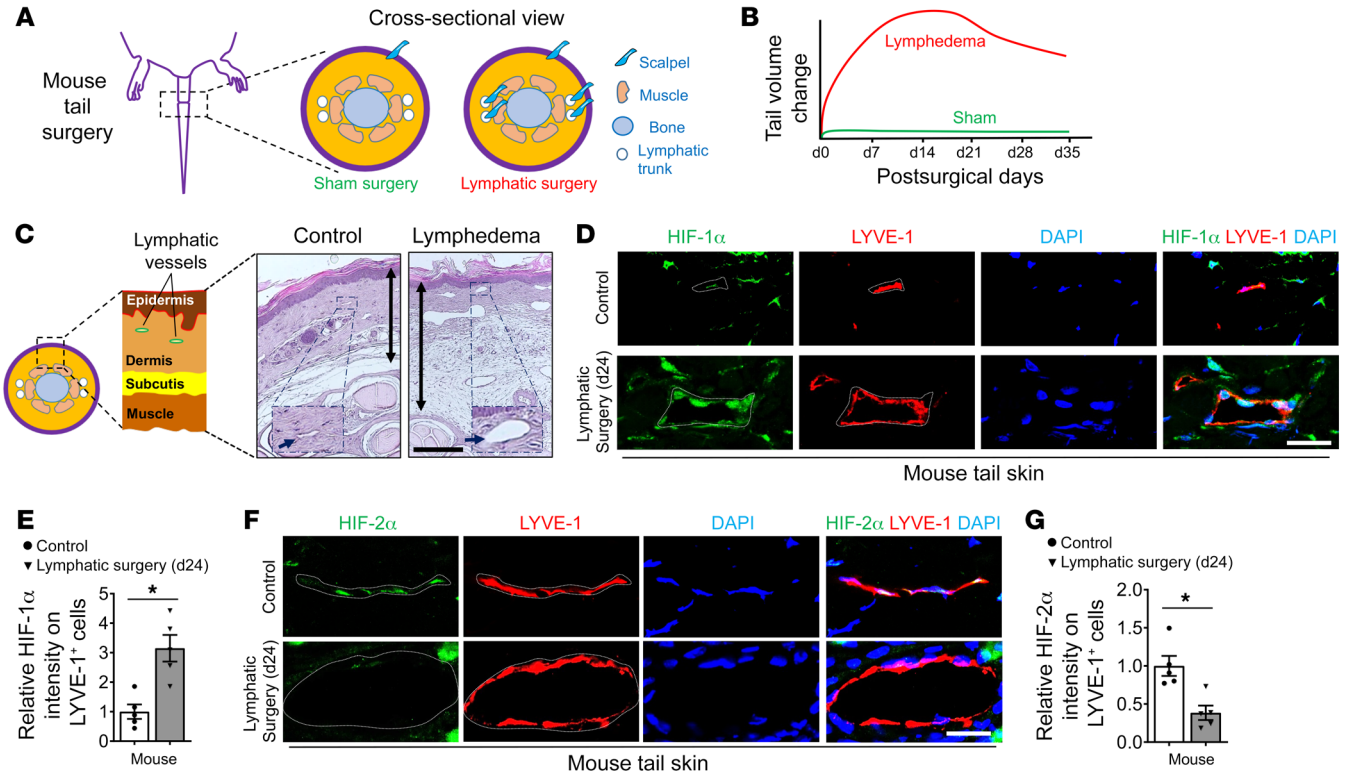

Figure 2. Increased HIF-1α and decreased HIF-2α expression in LECs of experimental mouse-tail lymphedema skin. (**A**) Mouse-tail model of acquired lymphedema. Sham surgery involves skin incision only; lymphatic surgery includes both skin incision and thermal ablation of lymphatic trunks. (**B**) Tail volume responses following sham or lymphatic surgery in a course of 35 days. The lymphedema tail volume response curve represents a maximal tail volume increase by d14–d21, followed by modest resolution. (**C**) A cartoon schematic showing mouse-tail skin histology, and a representative H&E staining of tail tissues harvested from control mice or mice subjected to lymphatic surgery. Insets in H&E images depict normal (control) or dilated lymphatic vessels. Black arrows point to lymphatic vessels in the insets. Double-headed black arrows illustrate the cutaneous layer. (**D**) Representative immunofluorescence staining of HIF-1α (green) and LYVE-1 (red) of the skin tissues harvested from control mice or animals subjected to lymphatic surgery. DAPI (blue) stains the nucleus. White dashed lines demarcate lymphatics. (**E**) Quantification of the HIF-1α intensity comparing groups shown in **D** (n = 5). (**F**) Representative immunofluorescence staining of HIF-2α (green) and LYVE-1 (red) of mouse skin samples. DAPI (blue) stains the nucleus. White dashed lines demarcate lymphatics. (**G**) Quantification of the HIF-2α intensity comparing groups shown in **F** (n = 5). In **E** and **G**, data are presented as mean ± SEM; *$P < 0.05$; by the Mann-Whitney test. n represents numbers of mice. Scale bars: 200 μm (**C**) and 30 μm (**D** and **F**).

tail swelling around d3–d9 with no observable differences by d14–d24 following lymphatic surgery (Supplemental Figure 8). LEC *Hif2α*-KO mice, by contrast, developed more severe tail swelling during the disease progression phase at all time points (Figure 3, A and B). Mice lacking LEC *Hif2α* responded to lymphatic injury with severe cutaneous thickening, pronounced lymphatic vascular remodeling, and an increased lymphatic area (Figure 3, C–E). Loss of *Hif2α* expression in blood endothelial cell (BECs) leads to downregulation of the adherens junctional protein, VE-Cadherin (20). We found reduced LEC VE-Cadherin expression in lymphedematous skin of LEC *Hif2α*-KO mice compared with that of the WT (Supplemental Figure 9). At d24 after lymphatic surgery, LEC *Hif2α*-deficient mice suffered poor lymphatic drainage through initial lymphatics and elevated lymphatic leakage as measured by near infrared (NIR) imaging (Figure 3, F–H), which likely result from dysfunctional primary lymphatic valves caused by decreased expression of VE-Cadherin. Thus, an exaggerated loss of HIF-2α, below that observed in disease, made lymphedema worse whereas reducing HIF-1α had relatively little effect.

Cell type–specific HIF-2α function has been previously illustrated to play important roles in health and disease (12). Lymphangiogenesis and lymphatic remodeling in lymphedema are regulated by prolymphangiogenic factors derived from myeloid cells (21). Macrophage-derived HIF-2α promotes M2 polarization, which influences tissue repair and remodeling (22–24). We therefore assessed the functional roles of HIF-2α expressed in the myeloid cell compartment in lymphedema development. Myeloid-specific *Hif2α* deletion was achieved through a previously established LysM-Cre–mediated breeding strategy (22, 23) (Supplemental Figure 10A). Our data show that LysM-Cre–specific *Hif2α* knockout did not alter tail responses in mice with sham surgery; instead, this gene deletion caused a transient tail volume increase on d14–d20 after lymphatic surgery, and tail swelling of myeloid *Hif2α*-deficient mice became indistinguishable from control mice by d24 after lymphatic surgery (Supplemental Figure 10, B and C). No exacerbated skin thickening nor lymphatic dilation were observed in myeloid *Hif2α*-deficient mice (Supplemental Figure 10, D and E). In summary, these data indicate that the loss of LEC-specific *Hif2α* accounts (more so than its loss in myeloid cells) for lymphatic remodeling, worsened lymphatic function, and exacerbated lymphedema; the low LEC HIF-2α observed in preclinical and clinical disease may consequently be an important pathogenic contributor to disease.

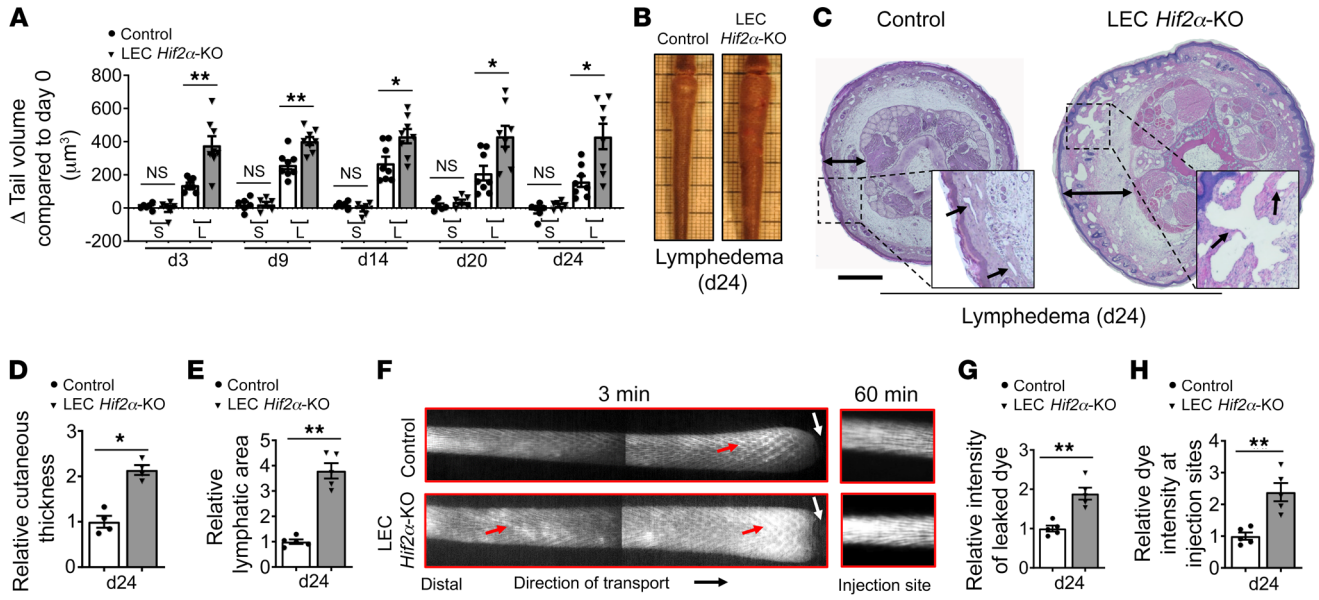

Figure 3. LEC *Hif2α*-KO augments tissue swelling and cutaneous skin thickness and exacerbates lymphatic malfunctioning. (**A**) Serial measurements of tail volume in WT and LEC *Hif2α*-KO mice with sham (n = 6) or lymphatic surgery (n = 8). L, lymphedema; S, sham. (**B**) Representative images of WT or LEC *Hif2α*-KO mouse tail 24d following lymphatic surgery. (**C**) Representative H&E staining of mouse-tail samples of WT or LEC *Hif2α*-KO mice subjected to lymphatic surgery. Black arrows point to dilated lymphatic vessels; double-headed black arrows illustrate the cutaneous thickness. (**D** and **E**) Quantification of cutaneous thickness (**D**) and lymphatic area (**E**) comparing groups shown in **C** (n = 4–5). (**F**) Representative NIR imaging of tails of WT and LEC *Hif2α*-KO mice after lymphatic surgery. Leaked NIR dye, IRDye 800CWNHS ester, was measured 3 minutes after injection. Two separate images were taken for the tail segment between the injection and surgical sites, and stitched for data presentation. Retained NIR dye was measured 60 minutes after injection. Red arrows point to interstitial area with dye leakage, white arrows point to surgical sites. (**G** and **H**) Quantification of the leaked (**G**) and retained (**H**) NIR dye intensity comparing the groups shown in **F** (n = 5). In **A**, **D**, **E**, **G**, and **H**, data are presented as mean ± SEM; $^*P < 0.05$; $^{**}P < 0.01$; by the Mann-Whitney test. n represents numbers of mice. Scale bar: 500 μm (**C**).

HIF-2α is required for lymphatic development and the maintenance of adult lymphatic vasculature. HIF-2α plays pivotal roles in the development of microvasculature and is essential for adult vascular maintenance (15, 25). We tested whether HIF-2α is required for lymphatic development, adopting a well-established protocol (26, 27), by analyzing embryonic dorsal skin lymphatic formation (Figure 4, A–C). Administration of tamoxifen at E10.5 and E11.5 effectively deleted LEC *Hif2α* (Supplemental Figure 11), and caused pronounced edema around the neck area of the dorsal skin of developing embryos (Figure 4D). Whole-mount staining of VEGFR3 indicated a greater gap between the leading edges of the growing dorsal lymphatics in the LEC *Hif2α*-KO embryos (Figure 4, E and F).

To test whether HIF-2α is also needed to sustain lymphatic homeostasis, dermal lymphatics were assessed after LEC *Hif2α* deletion in fully developed adult mice. Lymphatic capillaries appeared to be dilated after silencing *Hif2α* for 21 days (Supplemental Figure 12, A and B). In trachea, LEC *Hif2α* knockout also led to lymphatic dilation and abnormal sprouting (Supplemental Figure 12, C and D). Further, ear skin Evans blue test illustrated decreased lymphatic drainage and increased lymphatic leakage in LEC *Hif2α*-KO mice (Figure 4, G and H). Together, these data indicate that LEC HIF-2α is required for proper embryonic lymphatic development and maintenance of adult lymphatic structure and function.

Hif2α deletion impairs LEC TIE2 signaling in lymphedema. ANGPT/TIE2 signaling is required for lymphatic development and the maintenance of adult lymphatic vasculature (28, 29). Blood microvascular endothelium-derived HIF-2α regulates ANGPT1/TIE2 signaling to preserve airway structure and function (15). As a first step to investigate whether TIE2 signaling is regulated by HIF-2α in LECs, the expression and activation of TIE2 were determined. TIE2 expression was significantly diminished following lymphatic surgery and was further reduced in LEC *Hif2α*-KO mice (Figure 5, A and B). Activation of TIE2, measured by TIE2 phosphorylation (p-TIE2, Y992), was also decreased in both control and LEC *Hif2α*-KO lymphedematous tissue, with weaker p-TIE2 staining in samples lacking LEC *Hif2α* (Figure 5, C and D). These data suggest that loss of LEC HIF-2α leads to diminished lymphatic TIE2 expression and signaling, a pathological alteration that likely exacerbates lymphatic dysfunction and lymphedema progression. Consistent with this result, markedly decreased LEC TIE2 and p-TIE2 immunofluorescence in the dorsal skin of LEC *Hif2α*-KO embryos was also observed (Supplemental Figure 13). Collectively, LEC cell-autonomous HIF-2α expression appears to regulate lymphatic development and repair by controlling TIE2 signaling.

Exogenous ANGPT1 overcomes lymphatic injury, observed in low LEC HIF-2α conditions, by stimulating TIE2 signaling. Given the established role for TIE2 signaling in lymphatic health (28, 29), we sought to further characterize the relationship between lymphatic HIF-2α and TIE2. First, we asked whether supplying exogenous TIE2 ligands could alleviate HIF-2α deficiency–associated lymphedema exacerbation. We employed an adenovirus-mediated overexpression strategy to enhance the expression of 2 major TIE2 ligands, ANGPT1 (Ad*Angpt1*) and ANGPT2 (Ad*Angpt2*) (15). Ad*Angpt1* or Ad*Angpt2* viral particles were administered intra-

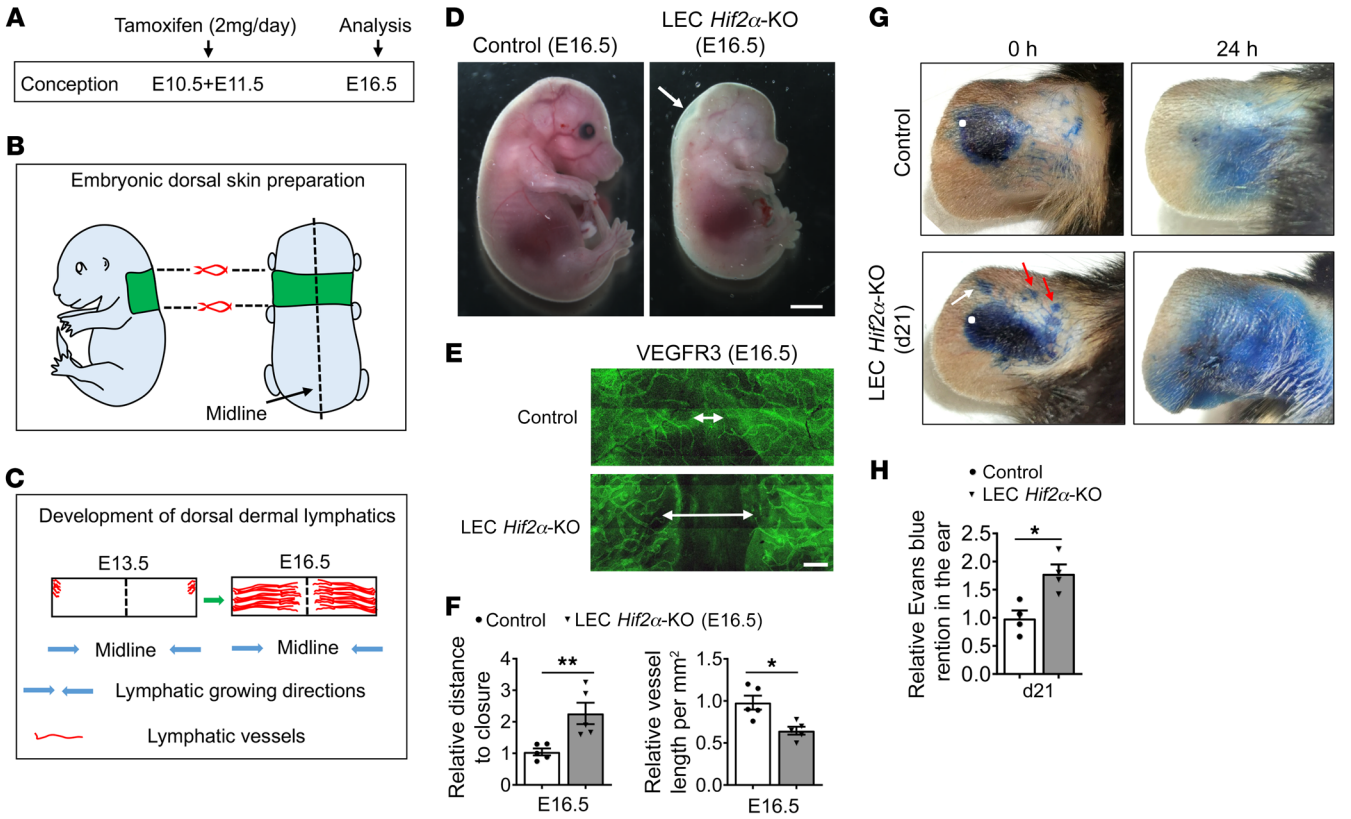

Figure 4. Deletion of lymphatic endothelial *Hif2α* impairs dermal lymphatic development and causes adult lymphatic abnormalities. (**A**) Experimental strategy for assessing the role of deleting LEC *Hif2α* in embryonic lymphatic development. (**B**) Location of the dorsal skin harvested. (**C**) Cartoon diagram of growth of lymphatics in the embryonic dorsal skin. (**D**) Bright field images of E16.5 control or LEC *Hif2α*-KO embryos. White arrow denotes lymphedema. (**E**) Representative E16.5 embryonic dorsal skin lymphatics stained by VEGFR3. Double arrow heads denote the distance between the leading fronts of lymphatic vessels. (**F**) Quantification of relative distance to closure and relative lymphatic length comparing groups shown in **E** (n = 5). (**G**) Representative photographs of ears at 0 and 24 hours after injection of Evans blue dye into control or LEC *Hif2α*-KO ears 21 days after tamoxifen administration. White dots denote injection sites. The white arrow points to retrograde lymph flow, red arrows point to areas with lymphatic leakage. (**H**) Extravasated dye was measured via absorbance at 620 nm, relative intensity of retained Evans blue was then calculated (n = 4). **F** and **H**, data are presented as mean ± SEM; $^*P < 0.05$; $^{**}P < 0.01$; by the Mann-Whitney test. n in **F** represents numbers of embryos from 2 litters, n in **H** represents numbers of mice. Scale bars: 2 mm (**D**) and 200 μm (**E**).

venously the same day as lymphatic surgery. Ad*Angpt1* therapy diminished tail swelling of mice lacking *Hif2α*, whereas Ad*Angpt2* treatment only transiently reduced tail edema (Figure 6, A and B). Cutaneous thickness and lymphatic dilation were notably improved after Ad*Angpt1* treatment, but no histological differences were detected in Ad*Angpt2* treatment groups in tissues harvested at d24 (Figure 6, C–E). ANGPT1 overexpression significantly improved lymphatic drainage and reduced lymphatic leakage, whereas the effect of increased ANGPT2 expression was limited (Figure 6, F–H). A similar trend of tail volume responses was observed in WT mice subjected to lymphatic injury following Ad*Angpt1* or Ad*Angpt2* treatment (Supplemental Figure 14); ANGPT1 alleviated lymphedema whereas ANGPT2 did not mitigate lymphedema in either *Hif2α*-deficient or WT mice.

Given the established agonistic role of ANGPT2 for lymphatic endothelium (30), we were surprised that Ad*Angpt1* was more effective than Ad*Angpt2* in ameliorating lymphedema in LEC *Hif2α*-KO mice, raising the possibility that altered ANGPT2 signaling occurs in lymphedema. In the blood vascular system, ANGPT1 plays an agonistic role in inflammatory conditions, whereas ANGPT2 becomes a TIE2 antagonist. TNF-α activation, in an inflammatory microenvironment, causes the shedding of the TIE1 ectodomain, leading to ANGPT2-mediated inactivation of TIE2 (Figure 7A and refs. 31, 32). To investigate whether, in lymphedema, lymphatic TIE2 activation could discriminate between the 2 adenoviral treatments, we evaluated TIE2 and p-TIE2 status in WT mice receiving either one of the adenoviral treatments after lymphatic surgery. Ad*Angpt1* increased both LEC TIE2 and p-TIE2 immunofluorescence in tails of mice subjected to lymphatic surgery; by contrast, administration of Ad*Angpt2* failed to increase TIE2 expression or activity (Figure 7, B–E). Based on these findings, in the context of lymphedema, ANGPT2 appears to be a less effective agonist of the lymphatic endothelium than it is under homeostatic conditions.

The attrition of TIE1 may be required for the dampening of TIE2 signaling in lymphedema (31, 32). We analyzed TIE1 expression in different experimental groups and observed strong expression in healthy lymphatics. LEC TIE1 was attenuated in lymphedema whereas overexpression of ANGPT1 partially restored TIE1 expression; ANGPT2 failed to correct TIE1 expression in

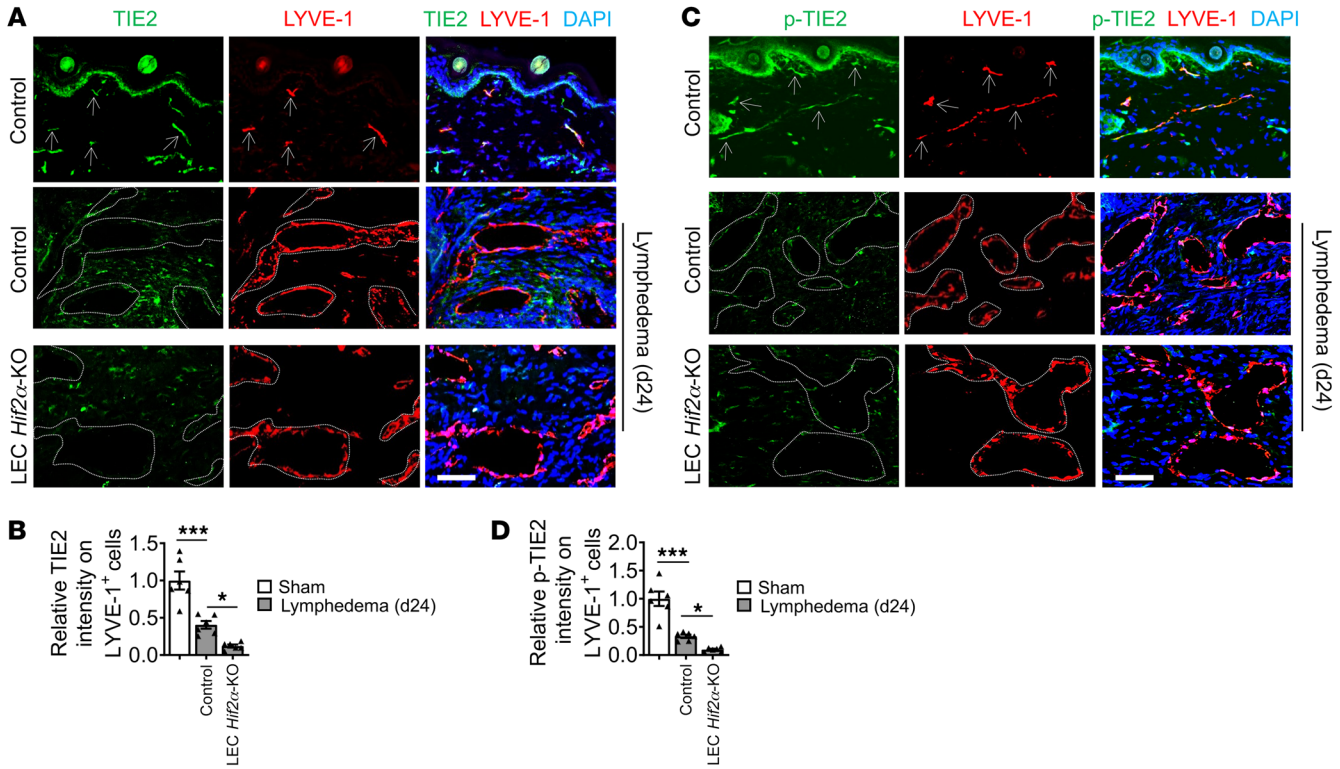

Figure 5. Deletion of lymphatic endothelial *Hif2α* diminishes LEC TIE2 signaling following lymphatic surgery. (**A**) Representative immunofluorescence staining of TIE2 (green) and LYVE-1 (red) of skin tissues harvested from sham groups or LEC *Hif2α*-KO mice with lymphatic surgery, compared to their littermate control. DAPI (blue) stains nucleus. White dashed lines demarcate dilated lymphatics. (**B**) Quantification of TIE2 intensity on LYVE-1$^+$ cells comparing the groups shown in **A** (n = 6). (**C**) Representative immunofluorescence staining of p-TIE2 (green) and LYVE-1 (red) of skin tissues harvested from sham groups or control and LEC *Hif2α*-KO mice with lymphatic surgery. DAPI (blue) stains nucleus. White dashed lines demarcate dilated lymphatics. (**D**) Quantification of p-TIE2 intensity on LYVE-1$^+$ cells comparing the groups shown in **C** (n = 6). In **B** and **D**, data are presented as mean ± SEM; $^*P < 0.05$; $^{***}P < 0.001$; by 1-way ANOVA followed by Tukey's post hoc test. n represents numbers of mice. Scale bars: 60 μm (**A** and **C**).

the dilated lymphatics of mice with lymphedema (Figure 8, A and B). To gain further insight into whether TNF-α expression correlates with the paucity of lymphatic TIE1, we assessed *Tnfα* transcripts. ANGPT1 treatment reduced the expression of TNF-α in the lymphedematous tissues, while Ad*Angpt2* therapy did not (Figure 8C). Pan-leukocyte marker CD45 staining indicated that Ad*Angpt1* reduced immune cell infiltration of the tail skin, in contrast to the Ad*Angpt2*-treated samples (Figure 8, D and E). Collectively, we demonstrate that in lymphedema, ANGPT1 promotes lymphatic repair and alleviates lymphedema through tonic activation of TIE2 signaling. Thus, in the low HIF-2α state of lymphedema, inflammation may reduce LEC TIE1 expression, an action that renders ANGPT2 less capable of activating TIE2 pathways.

Hif2α overexpression alleviates lymphedema and enhances protective TIE2 activity. Given that LEC-specific deletion of HIF-2α markedly exacerbates pathological lymphatic remodeling and tail swelling, we asked whether augmenting LEC HIF-2α expression improves lymphatic function and alleviates lymphedema. We generated inducible LEC-specific *Hif2α*-overexpressing (*Hif2α*-OE) mice, by crossing the Prox-1-CreERT2 mice with *LSLHif2α* mice as previously described (15, 33). LEC *Hif2α* overexpression resulted in increased LEC HIF-2α expression in the tail skin of mice (Supplemental Figure 5), and sustained LEC HIF-2α expression following lymphatic surgery (Supplemental Figure 15). LEC *Hif2α* overexpression reduced tail swelling in mice with lymphedema surgery (Figure 9, A and B). Augmented *Hif2α* in LECs reduced cutaneous thickness, prevented lymphatic remodeling, promoted solute uptake, and reduced lymphatic leakage (Figure 9, C–H). We next examined LEC TIE2 signaling in LEC *Hif2α*-OE mice with lymphatic injury. Increased LEC TIE2 was observed in the skin from the diseased *Hif2α*–OE mice (Figure 10, A and B). Using the adenovirus-mediated approach (15), we found that *Hif2α* overexpression fostered *TIE2* mRNA transcription in human-dermal (HD) LECs (Figure 10C), indicating that TIE2 may be a downstream target of HIF-2α. Higher expression of p-TIE2 was evident in LECs of tissues from LEC *Hif2α*-OE mice subjected to lymphatic surgery (Figure 10, D and E). Evaluation of TIE2 ligand expression illustrated that LEC HIF-2α overexpression restored *Angpt1*, but not *Angpt2*, in the skin from mice subjected to lymphatic surgery (Figure 10, F and G). Additionally, we found enhanced LEC TIE1 expression in LEC *Hif2α*-OE mice after lymphedema surgery (Figure 10, H and I) and significantly decreased *Tnfα* mRNA levels in *Hif2α*-OE mice subjected to lymphatic surgery (Figure 10J). There was also a marked reduction of CD45$^+$ inflammatory cell infiltration in the skin of LEC *Hif2α*-OE mice with lymphedema (Supplemental Figure 16). Together, our results indicate that lymphatic injury, edema and inflammation reduce LEC HIF-2α expression, which in turn leads to decreased TIE2 expression;

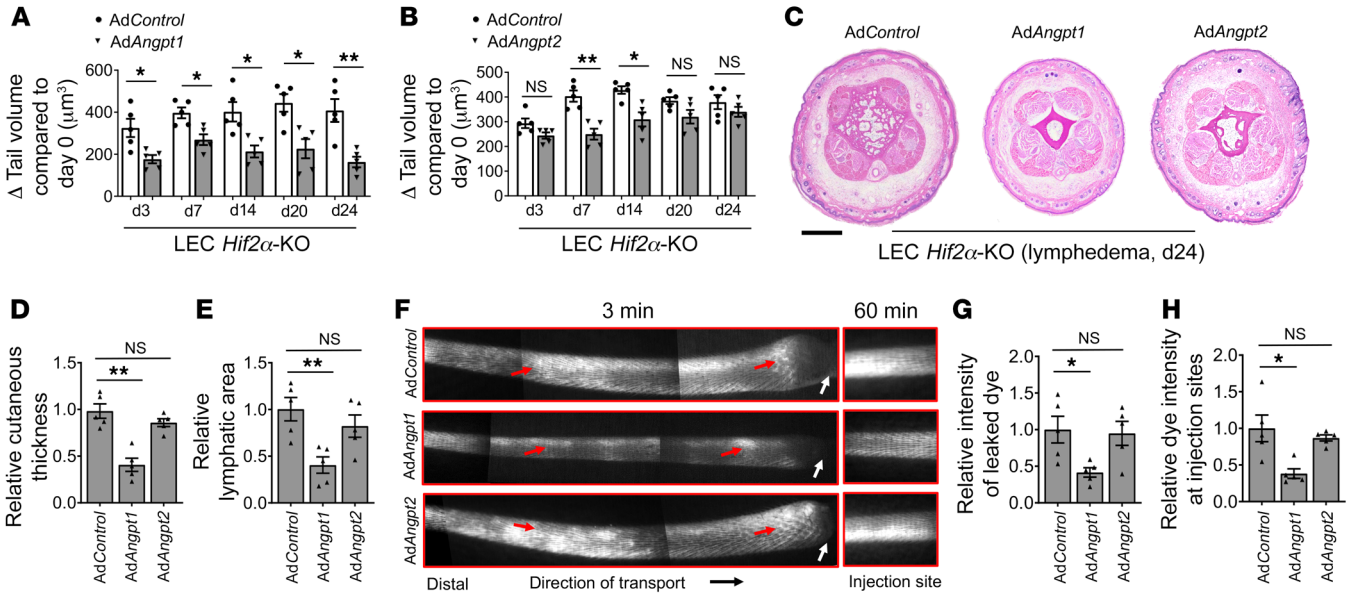

Figure 6. Ad*Angpt1* but not Ad*Angpt2* gene therapy attenuates lymphedema and improves lymphatic function in LEC *Hif2α*-KO mice following lymphatic injury. Adenoviral particles were injected intravenously on the same day when surgery was performed. LacZ adenovirus were administered as vector controls (Ad*Control*). (**A** and **B**) Quantitation of tail volume responses of lymphedema mice treated with Ad*Angpt1* (**A**) or Ad*Angpt2* (**B**) (n = 5). (**C**) Representative H&E staining of samples from the Ad*Control*-, Ad*Angpt1*-, or Ad*Angpt2*-treated mice with lymphatic surgery. (**D** and **E**) Quantification of cutaneous thickness (**D**) and lymphatic area (**E**) comparing groups shown in **C** (n = 5). (**F**) Representative NIR imaging of tails of Ad*Control*-, Ad*Angpt-1*, or Ad*Angpt2*-treated mice after lymphatic surgery. Leaked NIR dye, IRDye 800CWNHS ester, was measured 3 minutes after injection. Two to three separate images were taken for the tail segment between the injection and surgical sites and stitched for data presentation. Retained NIR dye was measured 60 minutes after injection. Red arrows point to interstitial areas with dye leakage, white arrows point to surgical sites. (**G** and **H**) Quantification of the leaked (**G**) and retained (**H**) NIR dye intensity comparing the groups shown in **F** (n = 5). In **A**, **B**, **D**, **E**, **G**, and **H**, data are presented as mean ± SEM; $^*P < 0.05$; $^{**}P < 0.01$; by the Mann-Whitney test (**A** and **B**) or Kruskal-Wallis test followed by Dunn's multiple comparisons test (**D**, **E**, **G**, and **H**). n represents numbers of mice. Scale bar: 500 μm (**C**).

together with reduced ANGPT1, increased ANGPT2, and loss of TIE1 (from TNF-α–mediated ectodomain shedding), LEC p-TIE2 is substantially downregulated. Lower TIE2 activity results in decreased VE-Cadherin expression. These molecular alterations compromise lymphatic drainage function and augment lymphatic leakage, which sustain edema as well as inflammation. Genetic overexpression of LEC HIF-2α leads to increased TIE2 expression and the restoration of TIE2 signaling; these in vivo responses are associated with restored ANGPT1 expression, reduced TNF-α production, and decreased TIE1 ectodomain shedding. Increased TIE2 activation in LEC *Hif2α*-OE mice with lymphedema results from a combined effect of increased TIE2, normalized ANGPT1, as well as a likely agonistic transition of ANGPT2 associated with restored TIE1 availability. Collectively, these changes correlate strongly with the resolution of lymphedema (Figure 11).

Discussion

In the United States, cancer and its treatment (particularly surgery and radiotherapy) are the major causes of secondary lymphedema, which now affects about 2 to 5 million cancer survivors (6, 34). No large-scale pharmaceutical trials have been performed, but emerging preclinical and clinical studies suggest that targeting inflammatory pathways may be effective (35–37). Lymphedema presents in heterogeneous conditions and should benefit from the characterization of actionable pathogenic mechanisms in experimental models. This study evaluated how HIFs, known factors for governing angiogenesis and maintaining blood vascular homeostasis, may regulate lymphatic pathophysiology in lymphedema. The results suggest that augmenting HIF-2α may have value in the treatment of lymphedema.

We first assessed LEC HIF-1α and HIF-2α expression in lymphedema skin and found markedly increased HIF-1α, but decreased HIF-2α expression in both clinical and preclinical tissues. Our data indicate that lymphedematous skin is hypoxic, consistent with the concept that excessive interstitial tissue fluid accumulation and inflammatory cell infiltrates increase tissue hypoxia, providing the stimulus for increased HIF-1α expression (11, 18, 38). The decline of LEC HIF-2α, however, appears counterintuitive, and suggests hypoxia-independent regulation of this HIF isoform. IFN-γ and endotoxin lipopolysaccharide (LPS) suppress HIF-2α expression in macrophages (23). LPS reduces HIF-2α expression in the lung (39). The airway parenchyma of a rejecting transplant is characterized by hypoxia and a reduction of HIF-2α (15). Together, these studies and our current findings support the notion that inflammatory mediators, particularly those attributable to Th1 immunity, may inhibit HIF-2α expression, even in the presence of significant tissue hypoxia. Further investigation is needed to uncover the precise molecular mechanisms that lead to divergent HIF isoform expression in LECs during lymphedema progression.

LEC-specific *Hif2α* deletion aggravated tail edema more profoundly than *Hif1α* deletion. HIF-1α is putatively beneficial to the lymphatics following injury by promoting VEGFR3 and VEGFC

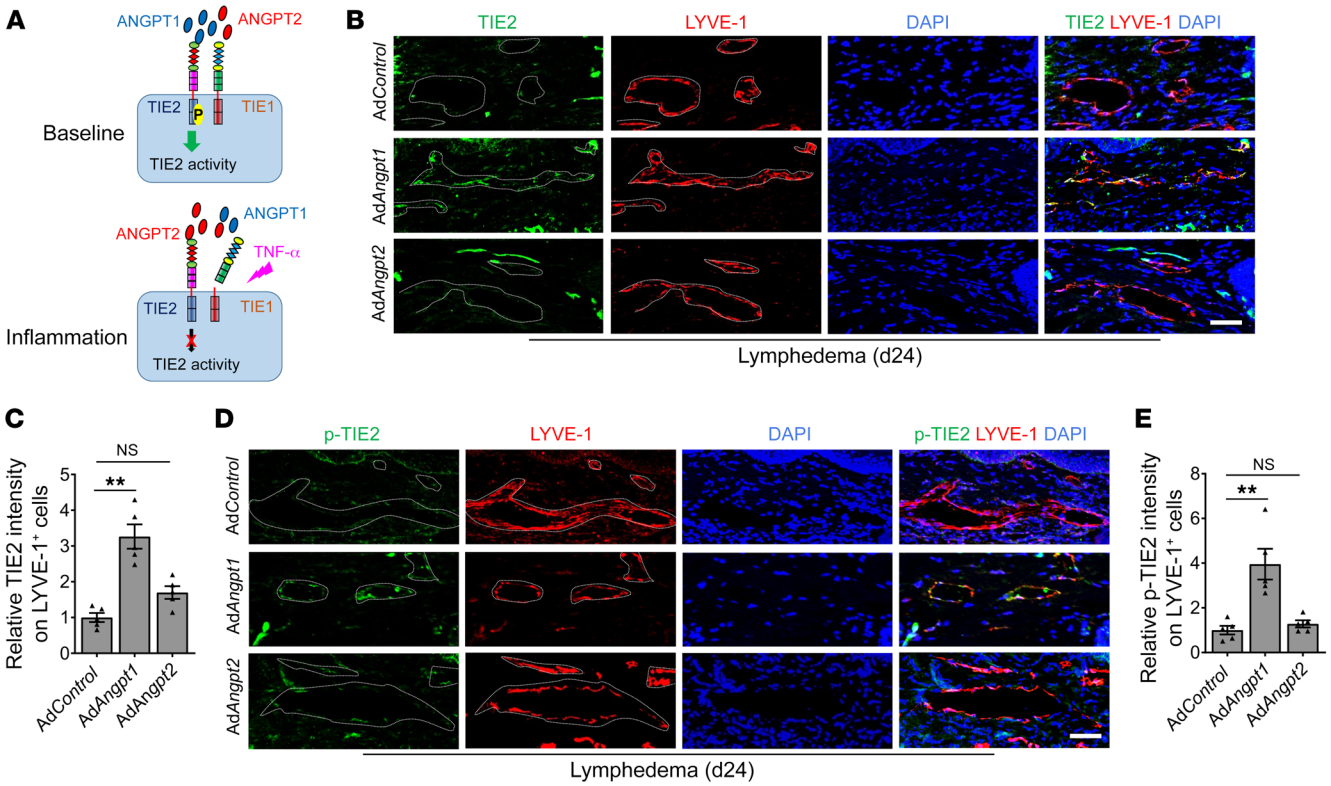

Figure 7. Ad*Angpt1* but not Ad*Angpt2* treatment enhances LEC TIE2 signaling after lymphatic injury. (**A**) Schematic showing previously reported working model of ANGPT1- or ANGPT2-mediated TIE2 activity in blood vascular endothelial cells. At baseline conditions, both ANGPT1 and ANGPT2 promote TIE2 phosphorylation (denoted by p); in inflammation, shedding of TIE1 ectodomain by TNF-α converts ANGPT2 into a TIE2 antagonist. (**B**) Representative immunofluorescence staining of TIE2 (green) and LYVE-1 (red) in skin tissues harvested from Ad*Control*-, Ad*Angpt1*-, or Ad*Angpt2*-treated mice with lymphatic surgery. DAPI (blue) stains nucleus. White dashed lines demarcate lymphatics. (**C**) Quantification of LEC TIE2 intensity comparing groups shown in **B** (n = 5). (**D**) Representative immunofluorescence staining of p-TIE2 (green) and LYVE-1 (red) in skin tissues harvested from Ad*Control*-, Ad*Angpt1*-, or Ad*Angpt2*- treated mice subjected to lymphatic surgery. DAPI (blue) stains nucleus. White dashed lines demarcate lymphatics. (**E**) Quantification of LEC p-TIE2 intensity comparing groups shown in **D** (n = 5). In **C** and **E**, data are presented as mean ± SEM; $^{**}P < 0.01$; by Kruskal-Wallis test followed by Dunn's multiple comparisons test. n represents numbers of mice. Scale bars: 60 μm (**B** and **D**).

expression in LECs and by enhancing VEGFC autocrine function (40); both actions are relevant during the early postsurgical period (18, 21). Systemic HIF-1α inhibition exacerbated tail swelling 3 weeks after lymphatic surgery (18), suggesting that HIF-1α expression in other cell types coordinates with LEC-derived HIF-1α to regulate lymphatic pathophysiology. LEC HIF-2α expression appears to be required for better lymphatic functioning following surgery, indicating that HIF-2α is essential for lymphatic repair. Loss of LEC HIF-2α potentiated pathological lymphatic sprouting and caused lymphatic dilation in lymphedema. These overgrown lymphatics are characterized by decreased expression of VE-Cadherin, an adherens junctional protein that is important for the formation of the button-like structure and the maintenance of the anatomical integrity of primary valves essential for interstitial fluid uptake as well as preventing retrograde lymph flow (41). In line with this result, NIR imaging of lymphedematous skin demonstrated drastically reduced fluid absorption capacity and increased leakage from lymphatic capillaries in LEC *Hif2α*-KO mice. HIF-2α in BECs stabilizes VE-Cadherin by upregulating vascular endothelial protein tyrosine phosphatase (VE-PTP) (20). However, because LECs lack VE-PTP expression (30), declining levels of LEC VE-Cadherin in LEC *Hif2α*-KO mice may result from reduced TIE2 activity. Conversely, TIE2 signaling promotes VE-Cadherin stability by activating PI3K and AKT, which in turn signal through Rac1 to inactivate RhoA (42). We recently showed how environmental exposure to tobacco smoke downregulates pulmonary endothelial HIF-2α (possibly contributing to the adult loss of gene expression and emphysema) (43). An emerging area of interest will be determining, in greater detail, how an acquired loss of LEC HIF-2α could similarly occur in developing lymphedema.

We studied the contribution of myeloid cell–expressed HIF-2α to lymphedema pathogenesis. Myeloid cell *Hif2α* deletion only transiently worsened tail swelling, suggesting that myeloid cell HIF-2α only regulates lymphatic functioning during the acute phase of lymphedema. Our results demonstrate that HIF-2α has cell context–dependent roles in lymphedema pathogenesis; LEC (rather than myeloid) HIF-2α appears to play the prominent role in promoting functional lymphatic remodeling in lymphedema.

The LEC-specific *Hif2α* loss- and gain-of-function genetic models demonstrate that HIF-2α regulates LEC TIE2 and p-TIE2 expression in lymphedema. The importance of TIE2 signaling in boosting blood vascular stability during inflammation is well documented (44), and its role for promoting lymphatic integrity was recently revealed (45). HIF-2α improved lymphatic structure

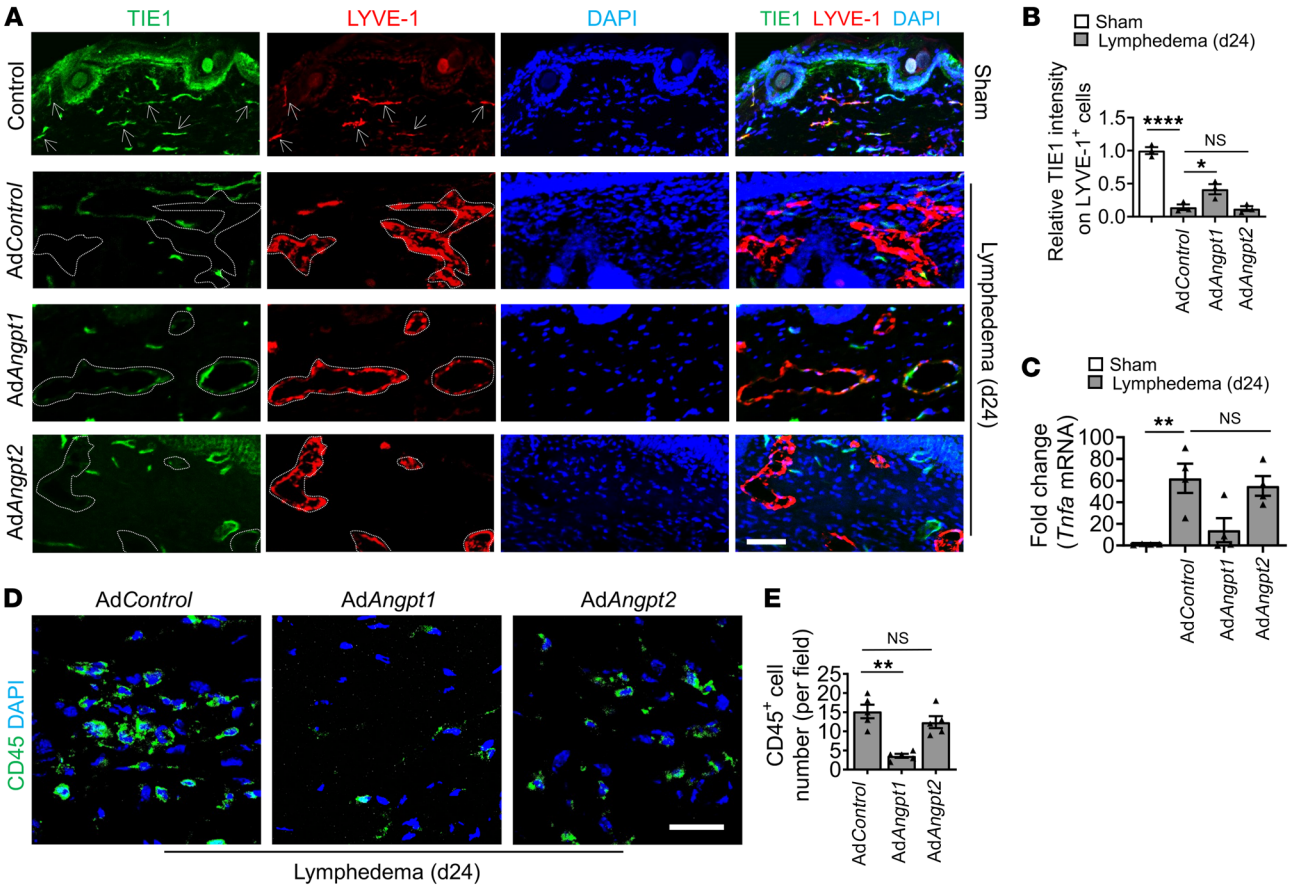

Figure 8. Ad*Angpt1* but not Ad*Angpt2* treatment enhances LEC TIE1 expression after lymphatic ablation. (**A**) Representative immunofluorescence staining of TIE1 (green) and LYVE-1 (red) in skin tissues harvested from WT sham control, or Ad*Control*-, Ad*Angpt1*-, or Ad*Angpt2*-treated mice with lymphatic surgery. DAPI (blue) stains nucleus. White dashed lines demarcate lymphatics. (**B**) Quantification of LEC TIE1 intensity comparing groups shown in **A** (n = 3). (**C**) Real time RT-PCR analysis of *Tnfα* mRNA expressed in tissues from WT sham control, or Ad*Control*-, Ad*Angpt1*-, Ad*Angpt2*-treated mice with lymphatic surgery (n = 4). (**D**) Representative immunofluorescence staining of CD45 (green) of dermal tissue of Ad*Control*-, Ad*Angpt1*-, or Ad*Angpt2*-treated mice with lymphatic surgery. DAPI (blue) stains nucleus. (**E**) Quantification of CD45$^+$ cells per field comparing groups shown in **D** (n = 5). In **B**, **C**, and **E**, data are presented as mean ± SEM; $^*P < 0.05$; $^{**}P < 0.01$; $^{****}P < 0.0001$; by ANOVA followed by Tukey's post hoc test. n represents numbers of mice. Scale bars: 60 μm (**A**) and 30 μm (**D**).

and functioning by enhancing LEC TIE2 signaling cascades. The increase of LEC p-TIE2 in lymphedematous skin of *Hif2α* gain-of-function mice compared with that of WT appears to be a combined effect of the following changes: (a) direct induction of TIE2 expression, also supported by previous analyses (15, 46, 47); (b) restored ANGPT1 expression; (c) decreased tissue TNF-α expression, resulting from reduced tissue inflammation; (d) restored TIE1 levels, because of reduced ectodomain shedding by TNF-α; and lastly, (e) a possible transition of ANGPT2 to TIE2 agonist because of higher TIE1 expression. Because ANGPT1 activates EC (including both BEC and LEC) TIE2 in a paracrine fashion (14), restored tissue ANGPT1 expression was probably attributable to augmented ANGPT1 expression by perivascular mesenchymal cells, rather than to a direct induction of ANGPT1 in LECs. LECs are known to scavenge inflammatory cytokines (48), but whether LEC HIF-2α overexpression can directly promote TNF-α scavenge is not known.

Like HIF-2α, LEC TIE2 expression was significantly reduced in lymphedema skin, a finding recapitulated in the blood endothelial cells (32). TIE2 reduction may be attributable to impaired lymph flow, given that the same occurs with reduced flow in blood vessels (49, 50). Flow dynamics and local inflammatory cytokine expression may control LEC HIF-2α protein expression and regulate TIE2 activation.

Overexpressing ANGPT1 increased TIE2 activation and ameliorated experimental lymphedema, whereas ANGPT2 overexpression was not effective. While ANGPT2 is generally considered to be a TIE2 antagonist in the blood vascular system (44), it serves as a TIE2 agonist in LECs (30, 51, 52). Overexpressing ANGPT2 was ineffective in promoting TIE2 phosphorylation at d24 after surgery, suggesting that ANGPT2 can only conditionally promote LEC TIE2 activity. In the blood vasculature, TNF-α–mediated shedding of TIE1 ectodomain during inflammation converts ANGPT2 into a TIE2 antagonist (31, 53). Here, LEC TIE1 was shed in lymphedema in association with rising TNF-α. The diminished impact of Ad*Angpt2* over time may be because of the rise of TNF-α and the loss of LEC TIE1. Although TIE1 may play an inhibitory role in regulating TIE2 signaling in vitro (54, 55), our result is consistent with recent findings suggesting that cell surface TIE1 expression is required for an agonistic effect of ANGPT2 in vivo (31, 32, 44).

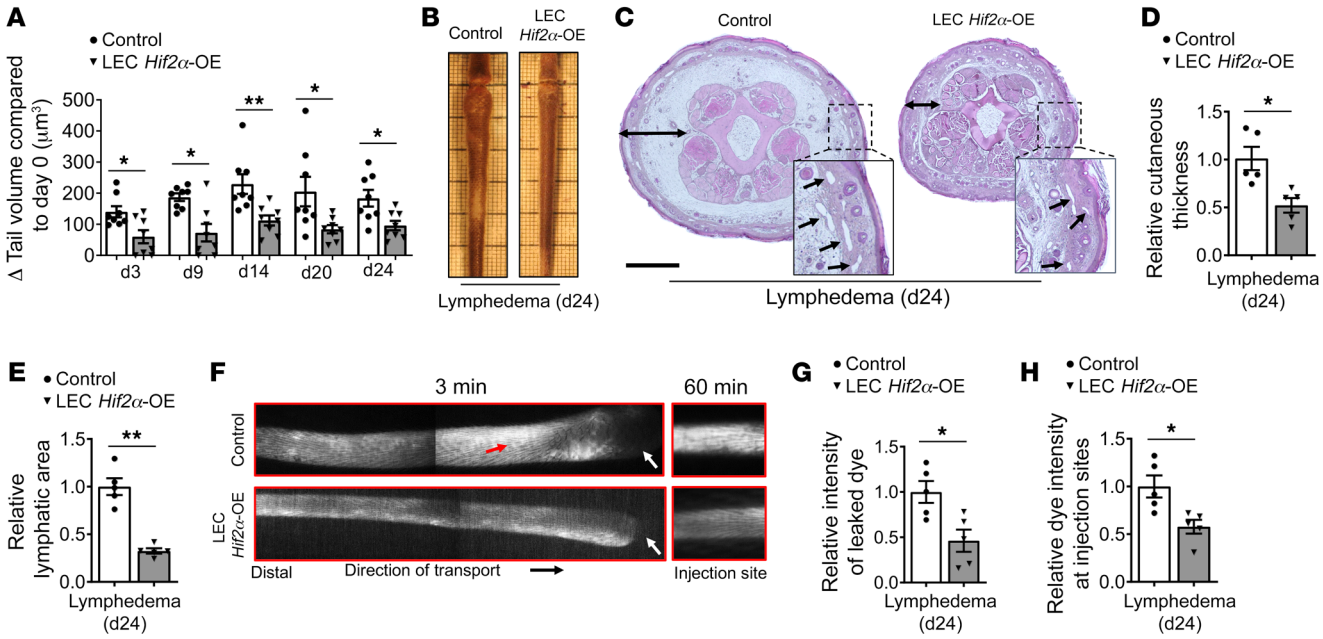

Figure 9. LEC *Hif2α*-OE mice subjected to lymphatic injury exhibit diminished tail swelling and improved lymphatic function. (**A**) Serial tail volume measurement of control and LEC *Hif2α*-OE mice with lymphatic surgery (n = 8). (**B**) Representative images of control or LEC *Hif2α*-OE tail 24 days following lymphatic surgery. (**C**) Representative H&E staining of tails of control or LEC *Hif2α*-OE mice with lymphatic surgery. Black arrows point to dilated lymphatics, double-headed black arrows illustrate the cutaneous thickness. (**D** and **E**) Quantification of cutaneous thickness (**D**) and lymphatic area (**E**) comparing groups shown in **C** (n = 5). (**F**) Representative NIR imaging of tails of control and LEC *Hif2α*-OE mice with lymphatic surgery. Leaked NIR dye, IRDye 800CWNHS ester, was measured 3 minutes after injection, 2 separate images were taken for the tail segment between the injection and surgical sites and stitched for data presentation. Retained NIR dye was measured 60 minutes after injection. Red arrow points to interstitial areas with dye leakage, white arrows point to surgical sites. (**G**, **H**) Quantification of the leaked (**G**) and retained (**H**) NIR dye intensity comparing the groups shown in **F** (n = 5). In **A**, **D**, **E**, **G**, and **H**, data are presented as mean ± SEM; $^*P < 0.05$; $^{**}P < 0.01$; by Mann-Whitney test. n represents numbers of mice. Scale bars: 500 μm (**C**).

Our data show that LEC-specific *Hif2α* deletion interfered with dorsal skin lymphatic development in embryos and caused abnormal lymphatic remodeling in adult mice. A marked decline of TIE2 and p-TIE2 immunofluorescence was observed in LECs of the developing embryo dorsal skin, indicating that LEC cell-autonomous HIF-2α expression may regulate lymphatic development by controlling TIE2 signaling. Activation of this latter pathway is required for normal lymphatic development and maintenance (29, 51, 52, 56, 57).

Our study has several limitations. For the TIE1 study, we only provided correlative evidence to indicate that intact TIE1 is critical for ANGPT2-mediated TIE2 activation in lymphedema. Future studies with LEC-specific *Tie1* knockouts will be necessary to definitively show that the agonistic effect of ANGPT2 requires the presence of TIE1 on LECs during inflammation. Absence of VE-PTP in LECs permits ANGPT2 to activate TIE2 signaling (30); whether and how VE-PTP expression may be altered in lymphedema requires further evaluation. The therapeutic effect of enhanced ANGPT1 for lymphedema may also be attributed to an effect on limiting blood vessel permeability and reducing the generation of interstitial fluid. Addressing this possibility will require the ongoing refinement of preclinical models. Future studies can also elucidate the function of HIF-2α in collecting lymphatics and whether HIF-2α and VEGFC/VEGFR3 signaling pathways converge to coordinate lymphangiogenesis and lymphatic remodeling.

In summary, this study provides both clinical and preclinical evidence that LEC HIF-2α is downregulated in lymphedema tissues. HIF-2α promotes functional lymphatic remodeling and drainage capacity and alleviates lymphedema through enhancement of TIE2 signaling. By contrast, LEC HIF-1α impacts lymphedema volume responses only transiently. Our data suggest that therapeutic augmentation of HIF-2α–mediated pathways are promising therapeutic avenues for lymphedema patients.

Methods

Mice. All mice were purchased from Jackson Laboratory. Detailed catalog information: C57BL/6J (B6; H-2^b), *Prox1*$^{tm3(cre/ERT2)Gco}$/J (Prox1-CreERT2), B6.129-Hif-1αtm3Rsjo/J (*Hif1α*$^{fl/fl}$), *Epas1*^{tm1Mcs}/J (*Hif2α*$^{fl/fl}$), B6.Cg-*Gt(ROSA)26Sor*$^{tm14(CAG-tdTomato)Hze}$/J (*LSLtdTomato*), B6.129S6(C)-*Gt(ROSA)26Sor*$^{tm4(HIF-2a*)Kael}$/J (*LSLHif2α*), B6.129P2-*Lyz2*$^{tm1(cre)Ifo}$/J (*LysM-Cre*). To create lymphatic endothelial specific knockout transgenic strains, mice expressing *Prox1-CreERT2* were crossed with *Hif2α*$^{fl/fl}$ or *Hif1α*$^{fl/fl}$ to achieve the following genotypes: LEC *Hif2α*-KO: *Prox1-CreERT2*, *Hif2α*$^{fl/fl}$ and LEC *Hif1α*-KO: *Prox1-CreERT2*, *Hif1α*$^{fl/fl}$. To create myeloid cell–specific *Hif2α* knockout strain, mice expressing LysM-Cre were crossed with mice with *Hif2α*$^{fl/fl}$ transgenes. To generate lymphatic endothelial gain-of-function transgenic strains, mice expressing *Prox1-CreERT2* were crossed with *LSLHif2α* to produce LEC *Hif2α*-OE: *Prox1-CreERT2*, *LSLHif2α*. *Cre*-mediated recombination of *LSLHif2α* leads to the expression of a *HIF-2α* variant that cannot be hydroxylated and degraded (33). Mice expressing *Prox1-CreERT2* were crossed with *LSLtdTomato* mice to generate reporter mice, in which LECs are labeled with tdTomato fluorescence. Cre-negative loxp-positive littermates were used as WT controls. Subcutaneous

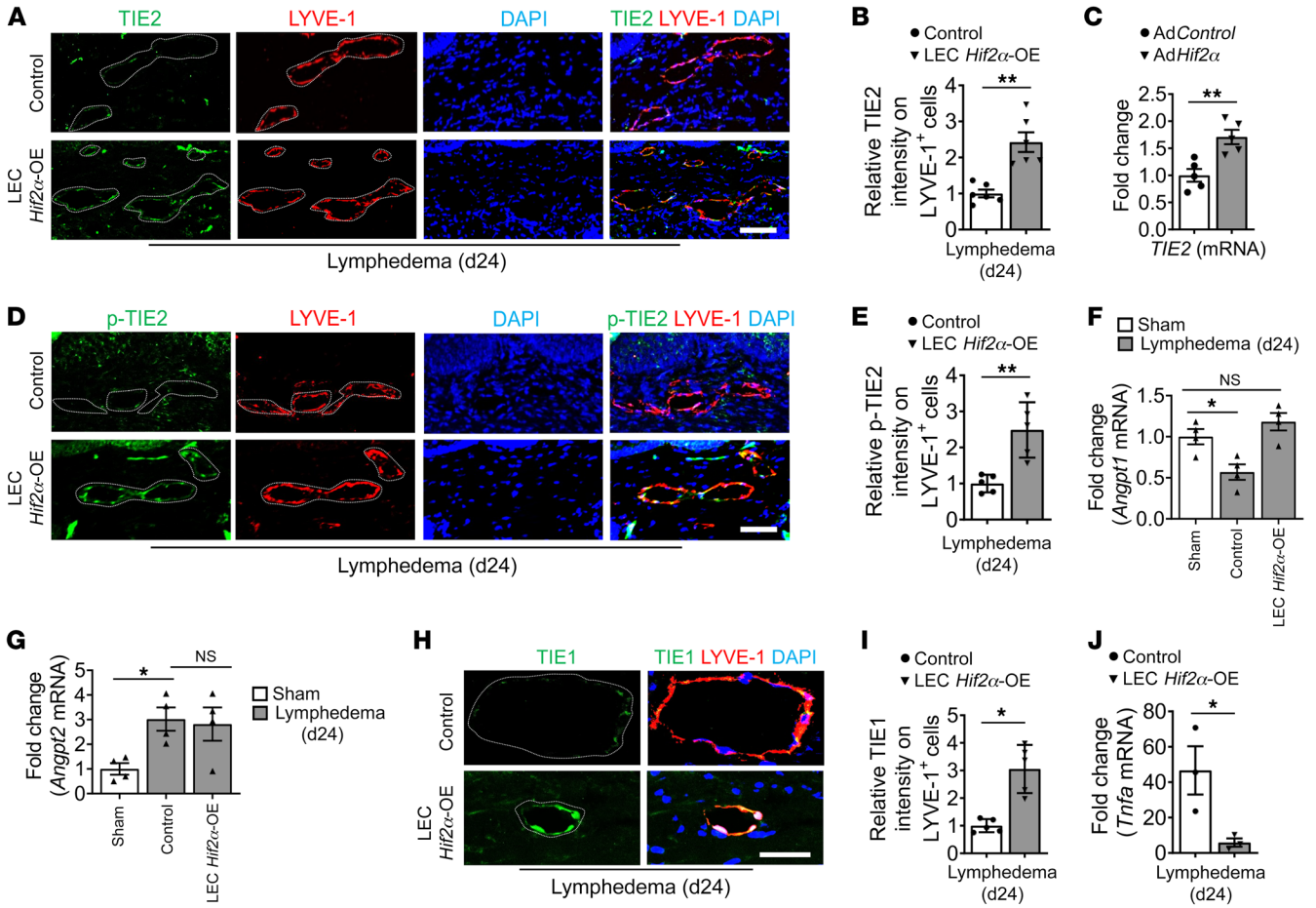

Figure 10. LEC-specific *Hif2α* overexpression enhances TIE2 signaling. (**A**) Representative immunofluorescence staining of TIE2 (green) and LYVE-1 (red) of skin tissues harvested from control and LEC *Hif2α*-OE mice with lymphatic surgery. DAPI (blue) stains nucleus. White dashed lines demarcate dilated lymphatics. (**B**) Quantification of TIE2 intensity on LYVE-1$^+$ cells comparing the groups shown in **A** (n = 6). (**C**) PCR analysis of TIE2 expression. HDLECs treated with adenoviral vector expressing *Hif2α* for 72 hours were subjected to RT-qPCR analysis. Empty viral vectors (Ad*Control*) were used as controls. (**D**) Representative immunofluorescence staining of p-TIE2 (green) and LYVE-1 (red) of skin tissues harvested from control and LEC *Hif2α*-OE mice with lymphatic surgery. DAPI (blue) stains nucleus. White dashed lines demarcate dilated lymphatics. (**E**) Quantification of p-TIE2 intensity on LYVE-1$^+$ cells comparing the groups shown in **D** (n = 5). (**F** and **G**) Real time RT-qPCR analysis of expression of *Angpt1* (**F**) or *Angpt2* (**G**) in skin tissues harvested from control or LEC *Hif2α*-OE mice. *Angpt1* and *Angpt2* expression in tissues with sham surgery was set as baseline (n = 4). (**H**) Representative immunofluorescence staining of TIE1 (green) and LYVE-1 (red) of skin tissues harvested from control and LEC *Hif2α*-OE mice with lymphatic surgery. DAPI (blue) stains nucleus. (**I**) Quantification of TIE1 intensity on LYVE-1$^+$ cells comparing groups shown in **H** (n = 5). (**J**) Real-time RT-qPCR analysis of *Tnfα* mRNA expressed in tissues from control or LEC *Hif2α*-OE mice subjected to lymphatic surgery (n = 3). In **B**, **C**, **E**–**G**, **I** and **J**, data are presented as mean ± SEM; $^*P < 0.05$; $^{**}P < 0.01$; by the Mann-Whitney test (**B**, **C**, **E**, **I**, and **J**) or by 1-way ANOVA followed by Tukey's post hoc test (**F** and **G**). n represents numbers of mice. Scale bars: 60 μm (**A** and **D**) and 30 μm (**H**).

injection of tamoxifen (Sigma, T5648) at a concentration of 200 mg/kg for 3 consecutive days was used to activate Cre activity. Age of mice used for experiments was 8 weeks.

Surgical induction of experimental lymphedema. Acquired lymphedema was surgically induced in tails of mice (including both males and females) through the thermal ablation of the lymphatic trunks and dermal lymphatic capillaries as previously described (17, 35). Briefly, a full-thickness-skin circumferential incision was made about 2 cm distal to the base of the mouse tail under anesthesia induced by ketamine (50 mg/kg) and xylazine (10 mg/kg) mixture. Lymphatic trunks were ablated through cautery. Mice of control sham surgery only received skin incision.

Tail volume quantification. Criteria for exclusion of mice for tail volume analysis were preestablished on the basis of our experience with this animal model. We excluded mice with self-inflicted mutilation or severe skin abrasion, severe infection, or tail necrosis because of loss of blood supply due to surgery. Tail images were taken through a digital photographic technique preoperatively (d0) and postoperatively (d3–d24), using an Olympus D-520 Zoom digital camera at high-quality resolution at a fixed distance from the subject. Tail volumes were calculated using the truncated cone approximation as we previously described (35).

Ear Evans blue drainage test. Mice were anesthetized with ketamine-xylazine mixture as used in the surgery, and 3 μL of 1% Evans blue dye solution (E2129, MilliporeSigma) was injected into both ears using tuberculin syringe. Pictures of ears were taken immediately and 24 hours after. Subsequently, the ears were collected for Evans blue dye extraction, following a previously established proto-

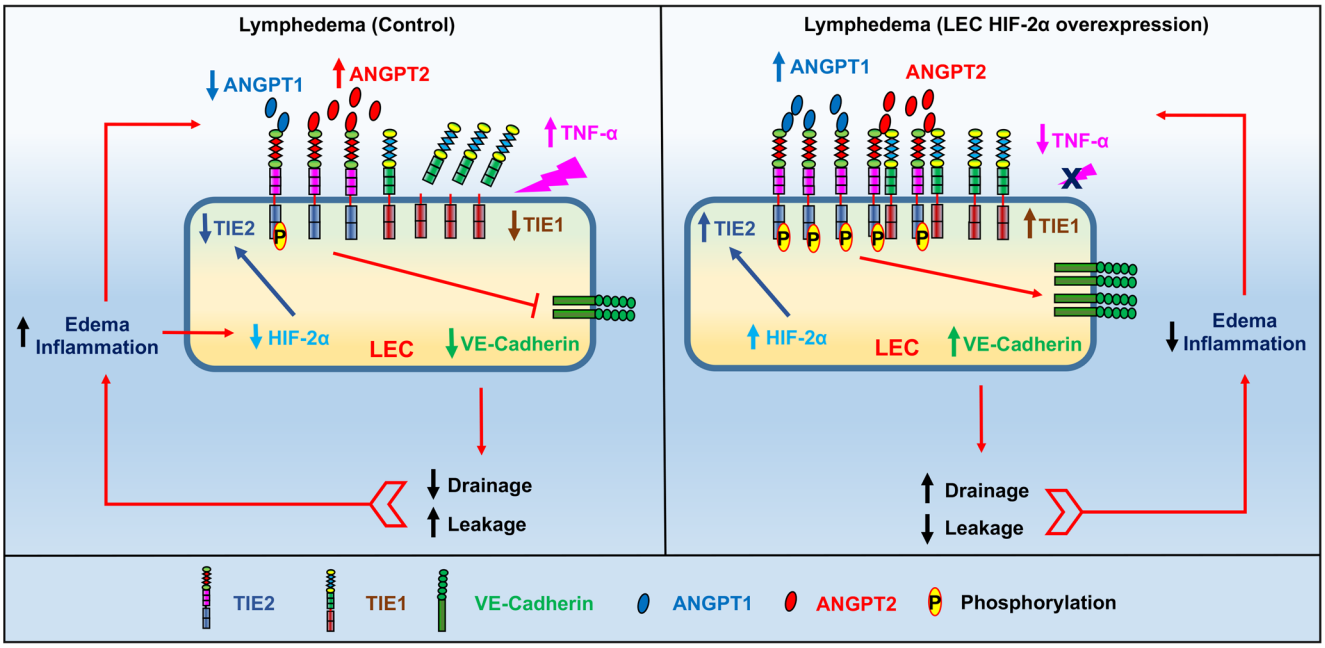

Figure 11. Schematic diagram showing LEC HIF-2α promotes lymphedema resolution by regulating TIE2 signaling. Lymphatic injury-caused edema and inflammation lead to reduced LEC HIF-2α expression, decreased tissue ANGPT1, increased ANGPT2 and TNF-α, and lower TIE1 expression (attributable to TNF-α–mediated ectodomain shedding). These changes collectively suppress LEC TIE2 activity and reduce the expression of the adherens junctional protein VE-Cadherin. Reduction of VE-Cadherin compromises lymphatic function, as evidenced by reduced interstitial drainage and increased lymphatic leakage, which exacerbates tissue edema and inflammation. When LEC HIF-2α is overexpressed, TIE2 and p-TIE2 expression increase, and lymphatic function, tissue inflammation, and edema improve. This resolution is accompanied by ANGPT1 restoration, declined TNF-α–mediated TIE1 shedding, and a possible agonistic switch wherein ANGPT2 strengthens LEC TIE2 signaling.

col (58). Briefly, dye was extracted from the ears by incubation for 2 days in 500 μL of formamide at 55°C with gentle, constant agitation. The amount of dye retained in the tissue was then determined by measuring the absorbance at 620 nm. Relative amount of retained dye was subsequently calculated.

Lymphatic drainage and leakage tests by NIR imaging. Lymphatic drainage and leakage tests were evaluated by NIR imaging and dye quantification as previously described (21, 59). Briefly, 10 μL IRDye 800CW NHS Ester conjugated to 40 KDa PEG (60) was injected intradermally; NIR images were taken 3 minutes or 60 minutes after dye injection by an Olympus microscopic imaging system (MVX10). ImageJ was used to evaluate dye intensity. Dye intensity obtained from the injection site was used to estimate dye retention, with higher intensity indicating compromised drainage. Intensity measured from the proximal interstitial areas were used to estimate lymphatic leakage. Relative intensities were calculated and presented.

Immunofluorescence staining. Frozen sections were used for immunohistochemistry. Tissues were snap-frozen in OCT solution (Sakura Finetek) after harvest. H&E or immunofluorescent staining was performed using 8 μm sections. Anti-LYVE-1 (1:50; LSBio catalog C106690) and anti-Gp38 (1:50; catalog M3619, Dako) antibodies were used to stain LECs. Other antibodies used included: anti-TIE2 (1:50; catalog AF762, R&D Systems), anti-p-TIE2 (recognizing the phosphorylation site Y992) (1:100; catalog AF2720, R&D Systems), anti-TIE1 (1:50; catalog AF619 R&D Systems), anti-CD45 (1:50; catalog 140451-81, eBioscience), anti-VEGFR3 (1:50; catalog AF743 R&D Systems), anti-HIF-1α (1:50; catalog NB100-449, Novus) and anti-HIF-2α (1:50; catalog NB100-122, Novus); anti-VE-Cadherin (1:50; catalog 550548, BD Bioscience). Secondary antibodies were labeled with the fluorochromes Alexa Fluor 488 or Alexa Fluor 594 (1:200; Invitrogen). Nuclei were stained with DAPI (Vector Laboratories). Photomicrographs were taken with a Zeiss LSM 710 laser scanning confocal microscope with Zeiss LSM Image Browser software. *Z*-stack was used to obtain low magnification images. In those experiments with cell number counting, stained cells were counted in 8 optical fields per section based on at least 5 sections from different samples.

Trachea and embryonic dorsal skin whole-mount immunofluorescence staining. Tracheas were harvested and fixed in 1% PFA in PBS for 1 hour at 4°C, followed by washing with PBS containing 0.1% Triton X-100, and 0.2% BSA. Tracheas were then permeabilized and stained with PBS containing 0.5% Triton X-100, 0.2% BSA, 0.1% sodium azide, and the primary antibody at the following dilution: LYVE-1 (1:500; catalog 11-034, AngioBio). Embryo skin was fixed in 4% PFA for 1 hour at 4°C. Samples were stained with VEGFR3 antibody (1:250, AF743, R&D Systems). Secondary antibody used was Alexa Fluor 488 (Jackson ImmunoResearch Laboratories). Samples were mounted with Vectashield Antifade Mounting Medium with DAPI. Slides were examined with a Zeiss LSM 710 Confocal Microscope using the Zen software.

Morphometric measurements. Quantification of the lymphatic area was carried out in the tile-scanned H&E images by using ImageJ as we previously described (35). Briefly, total area of the lymphatic vessel in a section was calculated and then compared. We also tested lymphatic quantification by using the immunofluorescence images (stained by LYVE-1), which showed an outcome comparable to the H&E images.

Quantification data presented were those using H&E images. For immunofluorescence staining quantification, HIF-1α, HIF-2α, TIE2, p-TIE2, TIE1, and VE-Cadherin intensity on LYVE-1$^+$ LECs were calculated as area density (total intensity/area); area refers to LYVE-1$^+$ LEC areas. Intensity was then normalized to control, which was set to 1. Number of infiltrated immune cells in tail skin with lymphedema surgery was quantified based on at least 6 high power fields per sample.

Real-time reverse transcription quantitative PCR (RT-qPCR). Tail skin samples were first incubated in RNAlater solution (Invitrogen) overnight at 4°C. Total RNA was then isolated using the RNeasy Fibrous Tissue Mini Kit (catalog 74704, Qiagen) following the manufacturer's protocol. For HDLEC (catalog C12217, MilliporeSigma) culture, cells were first detached from culture dishes and then collected. Total RNA was then isolated using the Qiagen Shredder (catalog 79654, Qiagen) and RNeasy Mini Kit (catalog 74104, Qiagen) following the manufacturer's protocol. RT-PCR was performed using FastStart SYBR Green (Roche) on a Lightcycler 480. mRNA expression relative to 18S mRNA expression was calculated using the delta-delta threshold cycle (ΔΔCT) method. PCR primers used: *TIE2*: CCCAAGCCTTCCAAAACGTG (forward), TTGCCCTCCCCAATCACATC (reverse); *Tnfa:* ATGGCCTCCCTCTCATCAGT (forward), ATAGCAAATCGGCTGACGGT (reverse); *Angpt1:* CTACCAACAACAACAGCATCC (forward), CTCCCT TTAGCAAAACACCTTC (reverse); *Angpt2:* CTGTGCGGAAATCTTCAAGTC (forward), TGC CATCTTCTCGGTGTT (reverse); *18S:* GAATCGAACCCTGATTCCCCGTC (forward), CGGCGACGACCCATTCGAAC (reverse).

Systemic adenovirus therapy. For ANGPT1, ANGPT2 overexpression experiments, adenoviral vectors expressing either ANGPT1 (Ad*Angpt1)* or ANGPT2 (Ad*Angpt2*) were intravenously injected retroorbitally same day as the lymphedema surgery was performed. Adenoviral vector expression LacZ (Ad*LacZ*) was used as control. The concentration of each type of virus used was 1×10^9 PFU as established by prior studies (15, 61).

Embryonic lymphatic development study. To induce Cre-mediated recombination during embryonic stage, pregnant mice were injected i.p. with 2 mg tamoxifen (MilliporeSigma, T5648) for 2 consecutive days (E10.5–E11.5). Skin tissues were harvested at E16.5. Standard whole-mount immunofluorescence staining procedure was carried out to stain the dorsal skin of the embryos. Images were taken by using Zeiss LSM 710 laser scanning confocal microscope with Zeiss LSM Image Browser software (as detailed above). Stitch imaging mode was chosen to image samples of large size. ImageJ was used to crop representative area from large, stitched images for data presentation. For quantification of lymphatic development in the dorsal skin, comparable regions between different samples were selected and cropped out for further analysis. ImageJ was used to measure relative distance to closure and relative lymphatic vessel length per mm^2 area.

Statistics. GraphPad Prism version 8.0 was used for statistical analysis. Differences between 2 groups at a single time point were compared using the Mann-Whitney test. For comparisons between multiple experimental groups at a single time point, Kruskal-Wallis test followed by Dunn's multiple comparisons test or 1-way ANOVA followed by Tukey's multiple comparison test were used. All analyses were considered statistically significant at P less than 0.05.

Study approval. All animal procedures were approved by Stanford's Administrative Panel on Laboratory Animal Care (APLAC) and the VA Palo Alto Institutional Animal Care and Use Committee (IACUC). Evaluation of human tissue was approved by the Stanford Institutional Review Board (protocol 7781). Adult patients with acquired lymphedema of upper extremity were assessed. Control samples were derived from the healthy contralateral limb of the same patient.

Author contributions

XJ, WT, EJG, and ABT planned and performed experiments and were responsible for data analysis. DK, PD, SP, GP, YK, AHL, FHE, and MC performed the experiments. JBD, SGR, and GLS provided intellectual input or reagents. XJ conceived the study. XJ, WT, and MRN wrote the manuscript. The order of the co–first authors was decided depending on the combined contribution of intellectual input and experiments performed.

Acknowledgments

This work was supported by NIH grants K12 HL120001-05 (to XJ), Stanford Chief Startup Funds, HL095686 and HL141105 (to MRN), and Stanford Endowed Chair Funds (to SRG and MRN).

Address correspondence to: Xinguo Jiang, VA Palo Alto Health Care System, Stanford University School of Medicine, 3801 Miranda Avenue, Building 101, A4-151, Palo Alto, California 94304, USA. Phone: 650.493.5000 ext. 64771; Email: xinguoj@stanford.edu. Or to: Mark R. Nicolls, VA Palo Alto Health Care System, Stanford University School of Medicine, 3801 Miranda Avenue, Med111P, Palo Alto, California 94304 USA. Phone: 650.493.5000 ext. 69289; Email: mnicolls@stanford.edu.

1. Jiang X, Nicolls MR, Tian W, Rockson SG. Lymphatic dysfunction, leukotrienes, and lymphedema. *Annu Rev Physiol*. 2018;80:49–70.
2. Schulze H, Nacke M, Gutenbrunner C, Hadamitzky C. Worldwide assessment of healthcare personnel dealing with lymphoedema. *Health Econ Rev*. 2018;8(1):10.
3. Grada AA, Phillips TJ. Lymphedema: pathophysiology and clinical manifestations. *J Am Acad Dermatol*. 2017;77(6):1009–1020.
4. Aspelund A, Robciuc MR, Karaman S, Makinen T, Alitalo K. Lymphatic system in cardiovascular medicine. *Circ Res*. 2016;118(3):515–530.
5. Paskett ED, Dean JA, Oliveri JM, Harrop JP. Cancer-related lymphedema risk factors, diagnosis, treatment, and impact: a review. *J Clin Oncol*. 2012;30(30):3726–3733.
6. Rockson SG, Keeley V, Kilbreath S, Szuba A, Towers A. Cancer-associated secondary lymphoedema. *Nat Rev Dis Primers*. 2019;5(1):22.
7. Semenza GL. Pharmacologic targeting of hypoxia-inducible factors. *Annu Rev Pharmacol Toxicol*. 2019;59:379–403.
8. Palazon A, Goldrath AW, Nizet V, Johnson RS. HIF transcription factors, inflammation, and immunity. *Immunity*. 2014;41(4):518–528.
9. Colgan SP, Furuta GT, Taylor CT. Hypoxia and innate immunity: keeping up with the HIFsters. *Annu Rev Immunol*. 2020;38:341–363.
10. Koh MY, Powis G. Passing the baton: the HIF switch. *Trends Biochem Sci*. 2012;37(9):364–372.
11. Lee P, Chandel NS, Simon MC. Cellular adaptation to hypoxia through hypoxia inducible factors and beyond. *Nat Rev Mol Cell Biol*. 2020;21(5):268–283.
12. Majmundar AJ, Wong WJ, Simon MC. Hypoxia-inducible factors and the response to hypoxic stress. *Mol Cell*. 2010;40(2):294–309.
13. Semenza GL. Oxygen sensing, homeostasis, and disease. *N Engl J Med*. 2011;365(6):537–547.
14. Eklund L, Kangas J, Saharinen P. Angiopoietin-Tie signalling in the cardiovascular and lymphatic systems. *Clin Sci*. 2017;131(1):87–103.
15. Jiang X, et al. Endothelial hypoxia-inducible factor-2α is required for the maintenance of airway microvasculature. *Circulation*. 2019;139(4):502–517.
16. Samanta D, Prabhakar NR, Semenza GL. Sys-

tems biology of oxygen homeostasis. *Wiley Interdiscip Rev Syst Biol Med*. 2017;9(4):e1382.
17. Tabibiazar R, et al. Inflammatory manifestations of experimental lymphatic insufficiency. *PLoS Med*. 2006;3(7):e254.
18. Zampell JC, Yan A, Avraham T, Daluvoy S, Weitman ES, Mehrara BJ. HIF-1α coordinates lymphangiogenesis during wound healing and in response to inflammation. *FASEB J*. 2012;26(3):1027–1039.
19. Schneider M, Ny A, Ruiz de Almodovar C, Carmeliet P. A new mouse model to study acquired lymphedema. *PLoS Med*. 2006;3(7):e264.
20. Gong H, et al. HIF2α signaling inhibits adherens junctional disruption in acute lung injury. *J Clin Invest*. 2015;125(2):652–664.
21. Rutkowski JM, Moya M, Johannes J, Goldman J, Swartz MA. Secondary lymphedema in the mouse tail: lymphatic hyperplasia, VEGF-C upregulation, and the protective role of MMP-9. *Microvasc Res*. 2006;72(3):161–171.
22. Imtiyaz HZ, et al. Hypoxia-inducible factor 2alpha regulates macrophage function in mouse models of acute and tumor inflammation. *J Clin Invest*. 2010;120(8):2699–2714.
23. Takeda N, et al. Differential activation and antagonistic function of HIF-{alpha} isoforms in macrophages are essential for NO homeostasis. *Genes Dev*. 2010;24(5):491–501.
24. Wynn TA, Vannella KM. Macrophages in tissue repair, regeneration, and fibrosis. *Immunity*. 2016;44(3):450–462.
25. Skuli N, et al. Endothelial deletion of hypoxia-inducible factor-2alpha (HIF-2alpha) alters vascular function and tumor angiogenesis. *Blood*. 2009;114(2):469–477.
26. Yu P, et al. FGF-dependent metabolic control of vascular development. *Nature*. 2017;545(7653):224–228.
27. Wong BW, et al. The role of fatty acid β-oxidation in lymphangiogenesis. *Nature*. 2017;542(7639):49–54.
28. Zheng W, Aspelund A, Alitalo K. Lymphangiogenic factors, mechanisms, and applications. *J Clin Invest*. 2014;124(3):878–887.
29. Kim J, et al. Impaired angiopoietin/Tie2 signaling compromises Schlemm's canal integrity and induces glaucoma. *J Clin Invest*. 2017;127(10):3877–3896.
30. Souma T, et al. Context-dependent functions of angiopoietin 2 are determined by the endothelial phosphatase VEPTP. *Proc Natl Acad Sci USA*. 2018;115(6):1298–1303.
31. Korhonen EA, et al. Tie1 controls angiopoietin function in vascular remodeling and inflammation. *J Clin Invest*. 2016;126(9):3495–3510.
32. Kim M, et al. Opposing actions of angiopoietin-2 on Tie2 signaling and FOXO1 activation. *J Clin Invest*. 2016;126(9):3511–3525.
33. Kim WY, et al. Failure to prolyl hydroxylate hypoxia-inducible factor alpha phenocopies VHL inactivation in vivo. *EMBO J*. 2006;25(19):4650–4662.
34. Rockson SG, Rivera KK. Estimating the population burden of lymphedema. *Ann N Y Acad Sci*. 2008;1131:147–154.
35. Tian W, et al. Leukotriene B_4 antagonism ameliorates experimental lymphedema. *Sci Transl Med*. 2017;9(389):eaal3920.
36. Gardenier JC, et al. Topical tacrolimus for the treatment of secondary lymphedema. *Nat Commun*. 2017;8:14345.
37. Rockson SG, et al. Pilot studies demonstrate the potential benefits of antiinflammatory therapy in human lymphedema. *JCI Insight*. 2018;3(20):e123775.
38. Poeze M. Tissue-oxygenation assessment using near-infrared spectroscopy during severe sepsis: confounding effects of tissue edema on StO2 values. *Intensive Care Med*. 2006;32(5):788–789.
39. Zeng H, He X, Tuo QH, Liao DF, Zhang GQ, Chen JX. LPS causes pericyte loss and microvascular dysfunction via disruption of Sirt3/angiopoietins/Tie-2 and HIF-2α/Notch3 pathways. *Sci Rep*. 2016;6:20931.
40. Min Y, Ghose S, Boelte K, Li J, Yang L, Lin PC. C/EBP-δ regulates VEGF-C autocrine signaling in lymphangiogenesis and metastasis of lung cancer through HIF-1α. *Oncogene*. 2011;30(49):4901–4909.
41. Baluk P, et al. Functionally specialized junctions between endothelial cells of lymphatic vessels. *J Exp Med*. 2007;204(10):2349–2362.
42. Milam KE, Parikh SM. The angiopoietin-Tie2 signaling axis in the vascular leakage of systemic inflammation. *Tissue Barriers*. 2015;3(1–2):e957508.
43. Pasupneti S, et al. Endothelial HIF-2α as a key endogenous mediator preventing emphysema [published online June 9, 2020]. *Am J Respir Crit Care Med*. https://doi.org/10.1164/rccm.202001-0078oc.
44. Parikh SM. Angiopoietins and Tie2 in vascular inflammation. *Curr Opin Hematol*. 2017;24(5):432–438.
45. Kajiya K, et al. Promotion of lymphatic integrity by angiopoietin-1/Tie2 signaling during inflammation. *Am J Pathol*. 2012;180(3):1273–1282.
46. Schlaeger TM, et al. Uniform vascular-endothelial-cell-specific gene expression in both embryonic and adult transgenic mice. *Proc Natl Acad Sci USA*. 1997;94(7):3058–3063.
47. Tian H, McKnight SL, Russell DW. Endothelial PAS domain protein 1 (EPAS1), a transcription factor selectively expressed in endothelial cells. *Genes Dev*. 1997;11(1):72–82.
48. Schwager S, Detmar M. Inflammation and lymphatic function. *Front Immunol*. 2019;10:308.
49. Kurniati NF, et al. The flow dependency of Tie2 expression in endotoxemia. *Intensive Care Med*. 2013;39(7):1262–1271.
50. Li R, Zijlstra JG, Kamps JA, van Meurs M, Molema G. Abrupt reflow enhances cytokine-induced proinflammatory activation of endothelial cells during simulated shock and resuscitation. *Shock*. 2014;42(4):356–364.
51. Dellinger M, et al. Defective remodeling and maturation of the lymphatic vasculature in Angiopoietin-2 deficient mice. *Dev Biol*. 2008;319(2):309–320.
52. Gale NW, et al. Angiopoietin-2 is required for postnatal angiogenesis and lymphatic patterning, and only the latter role is rescued by Angiopoietin-1. *Dev Cell*. 2002;3(3):411–423.
53. Singh H, Hansen TM, Patel N, Brindle NP. The molecular balance between receptor tyrosine kinases Tie1 and Tie2 is dynamically controlled by VEGF and TNFα and regulates angiopoietin signalling. *PLoS ONE*. 2012;7(1):e29319.
54. Song SH, Kim KL, Lee KA, Suh W. Tie1 regulates the Tie2 agonistic role of angiopoietin-2 in human lymphatic endothelial cells. *Biochem Biophys Res Commun*. 2012;419(2):281–286.
55. Seegar TC, et al. Tie1-Tie2 interactions mediate functional differences between angiopoietin ligands. *Mol Cell*. 2010;37(5):643–655.
56. Zheng W, et al. Angiopoietin 2 regulates the transformation and integrity of lymphatic endothelial cell junctions. *Genes Dev*. 2014;28(14):1592–1603.
57. Thomson BR, et al. A lymphatic defect causes ocular hypertension and glaucoma in mice. *J Clin Invest*. 2014;124(10):4320–4324.
58. Escobedo N, et al. Restoration of lymphatic function rescues obesity in Prox1-haploinsufficient mice. *JCI Insight*. 2016;1(2):e85096.
59. Weiler M, Dixon JB. Differential transport function of lymphatic vessels in the rat tail model and the long-term effects of Indocyanine Green as assessed with near-infrared imaging. *Front Physiol*. 2013;4:215.
60. Nelson TS, et al. Lymphatic remodelling in response to lymphatic injury in the hind limbs of sheep. *Nat Biomed Eng*. 2020;4(6):649–661.
61. Thurston G, et al. Angiopoietin-1 protects the adult vasculature against plasma leakage. *Nat Med*. 2000;6(4):460–463.